Low-Energy $\bar{K}N$ and Pion-Hyperon Interactions. II. Applications of the K-Matrix Analysis*

B. R. MARTIN
Department of Physics, University College, London, England
AND
M. SAKITT
Brookhaven National Laboratory, Upton, New York 11973
(Received 18 March 1969)

s-wave K-matrix parameters deduced from a previous analysis of K^-p data are used to obtain the scattering lengths and low-energy behavior of the s-wave $\bar{K}N$, $\pi\Lambda$, and $\pi\Sigma$ amplitudes. In addition, an application involving the use of KN forward-dispersion-relation sum rules to calculate values for the $K\Lambda N$ and $K\Sigma N$ coupling constants is given. We show that present ambiguities in the evaluation of the unphysical regions of these sum rules prevent a reliable calculation of the coupling constants being made at this time. We conclude that $3 \lesssim g^2_{K\Lambda p}/4\pi \lesssim 15$ and $g^2_{K\Sigma^0 p}/4\pi \lesssim 2.1$.

1. INTRODUCTION

IN the preceding paper[1] we presented an analysis of K^-p scattering data in the kaon laboratory momentum range $k_L \lesssim 300$ MeV/c using an s-wave K-matrix formulation. It was shown that a good fit to all the available data could be obtained in a zero-range approximation involving nine real parameters. The values of these parameters and their associated errors were given. In this paper, we will use the K-matrix parameters to obtain the behavior of the $\bar{K}N$, $\pi\Lambda$, and $\pi\Sigma$ s-wave amplitudes and, in addition, to discuss an application involving the use of kaon-nucleon forward-dispersion-relation sum rules to calculate values for the $K\Lambda N$ and $K\Sigma N$ coupling constants.

In Sec. 2, devoted to the $\bar{K}N$ interaction, we discuss the behavior of the $I=0$ and 1 amplitudes in the low-energy physical region and in the unphysical region below the $\bar{K}N$ threshold. Values are given for the $I=0$ and 1 s-wave scattering lengths and the parameters of the $Y_0^*(1405)$ resonance. Section 3 contains a similar discussion for the $\pi\Lambda$ and $\pi\Sigma$ scattering amplitudes, and in Sec. 4 we discuss the evaluation of the kaon-hyperon coupling constants from forward-dispersion-relation sum rules. Finally, Sec. 5 contains a summary of the calculations.

2. KN INTERACTIONS

A. $I=1$ Scattering

We shall define the s-wave $I=1$ $\bar{K}N$ scattering amplitude $f_1^N(W)$ by

$$f_1^N(W)=\frac{A_1(W)}{1-ikA_1(W)}, \tag{1}$$

where k is the magnitude of the center-of-mass three-momentum in the $\bar{K}N$ system, W is the total center-of-mass energy, and $A_1(W)$ is defined in terms of the K-matrix elements by Eqs. (8)–(13) of I. Graphs of $\mathrm{Re}f_1^N(W)$ and $\mathrm{Im}f_1^N(W)$ as a function of W are shown in Fig. 1. The continuation of the various momenta below their respective thresholds is affected by letting $q \to i|q|$. The amplitudes are small in both the physical and unphysical regions, and show no significant structure apart from the necessary cusps at the $\pi\Sigma$ and $\bar{K}N$ thresholds.[2]

Above the $\bar{K}N$ threshold, $f_1^N(W)$ may be written in terms of a complex phase shift $\alpha_1^N(W)$ by

$$f_1^N(W)=\frac{\exp[2i\alpha_1^N(W)]-1}{2ik}=\frac{\eta_1^N(W)\exp[2i\delta_1^N(W)]}{2ik}, \tag{2}$$

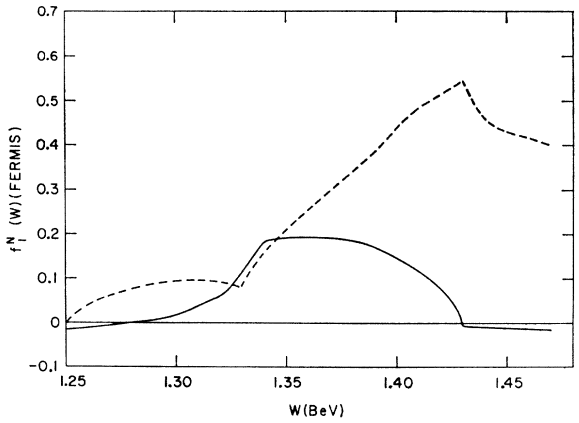

FIG. 1. $\bar{K}N$ scattering amplitude for the isotopic-spin $I=1$ channel plotted as a function of the total center-of-mass energy W. The dotted curve is the imaginary part and the solid curve is the real part of the scattering amplitude.

* Work performed under the auspices of the U. S. Atomic Energy Commission.

[1] B. R. Martin and M. Sakitt, preceding paper, Phys. Rev. 183, 1345 (1969), hereinafter called I.

[2] Throughout this paper we shall consider amplitudes for a definite isospin. We shall therefore neglect the small $K^0K^\pm$ mass difference, so that there will be no cusps at the $\bar{K}^0n$ threshold.

TABLE I. Values of the s-wave $I=1$ $\bar{K}N$ scattering length (in F) as calculated by various authors, and the result of this paper.

$A_1 \equiv a_1 + ib_1$	Method	Ref.
$(0.00\pm0.06)+i(0.69\pm0.03)$	Constant scattering length analysis for $k_L \lesssim 300$ MeV/c	3
$(-0.19\pm0.08)+i(0.44\pm0.04)$	Constant scattering length analysis for $k_L \lesssim 300$ MeV/c	4
$(-0.13\pm0.02)+i(0.51\pm0.03)$	Effective range K-matrix analysis for $k_L \lesssim 550$ MeV/c	5
$(-0.09\pm0.03)+i(0.54\pm0.02)$	Zero-range K-matrix analysis for $k_L \lesssim 300$ MeV/c	Present calculation

where

$$\eta_1^N(W) = \exp[-2\,\mathrm{Im}\alpha_1^N(W)] \tag{3}$$

and

$$\delta_1^N(W) = \mathrm{Re}\alpha_1^N(W). \tag{4}$$

Graphs of $\delta_1^N(W)$ and the inelasticity factor $\eta_1^N(W)$ are shown in Fig. 2. The real part of the phase shift is small and negative throughout the low-energy region, with the inelasticity becoming increasingly stronger.

Finally, the s-wave $I=1$ $\bar{K}N$ scattering length may be found by evaluating Eq. (1) at $k=0$. The result is given in Table I together with its error, which has been found using the K-matrix errors given in I. Table I also shows, for comparison, some previous determinations of this scattering length.[3–5] The agreement between the various calculations is satisfactory.

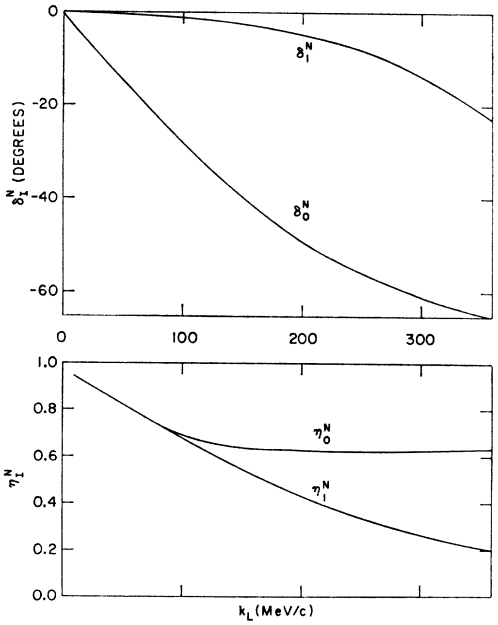

FIG. 2. Phase shift δ_I^N and inelasticity η_I^N for the $\bar{K}N$ system for both isotopic-spin $I=1$ and 0 channels plotted as a function of the laboratory momentum of the kaon k_L.

[3] J. K. Kim, Phys. Rev. Letters **14**, 29 (1965).
[4] M. Sakitt, T. B. Day, R. G. Glasser, N. Seeman, J. Friedman, W. E. Humphrey, and R. R. Ross, Phys. Rev. **139**, B719 (1965).
[5] F. von Hippel and J. K. Kim, Phys. Rev. Letters **20**, 1303 (1968).

B. $I=0$ Scattering

By analogy with $I=1$ $\bar{K}N$ scattering, we will define an s-wave amplitude for $I=0$ scattering by

$$f_0^N(W) = \frac{A_0(W)}{1-ikA_0(W)}, \tag{5}$$

where $A_0(W)$ is given in terms of the K-matrix elements by Eqs. (4) and (5) of I. Graphs of $\mathrm{Re}f_0^N(W)$ and $\mathrm{Im}f_0^N(W)$ as a function of W are shown in Fig. 3. Both $\mathrm{Re}f_0^N(W)$ and $\mathrm{Im}f_0^N(W)$ are very large in the unphysical region below the $\bar{K}N$ threshold (a point which will be discussed further in Sec. 4), $\mathrm{Im}f_0^N(W)$ having a maximum value at $W=1413$ MeV, at which point $\mathrm{Re}f_0^N(W)$ has a zero. We shall see later that this pole is associated with the existence of the $Y_0^*(1405)$ resonance.

Above the $\bar{K}N$ threshold, we may write, by analogy with Eq. (2),

$$f_0^N(W) = \frac{\eta_0^N(W)\exp[2i\delta_0^N(W)]-1}{2ik}, \tag{6}$$

and graphs of $\delta_0^N(W)$ and $\eta_0^N(W)$ are given in Fig. 2. The real part of the phase shift $\delta_0^N(W)$ is large and increasingly negative throughout the low-energy region,

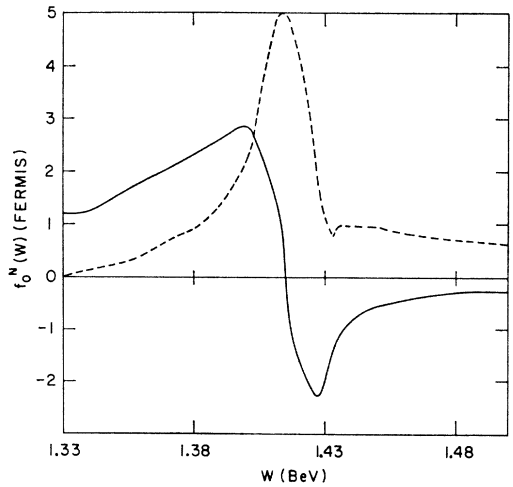

FIG. 3. $\bar{K}N$ scattering amplitude for the isotopic-spin $I=0$ channel plotted as a function of the total center-of-mass energy W. The dotted curve is the imaginary part and the solid curve is the real part of the scattering amplitude.

TABLE II. Values of the s-wave $I=0$ $\bar{K}N$ scattering length (in F) as calculated by various authors, and the result of this paper.

$A_0 \equiv a_0 + ib_0$	Method	Ref.
$(-1.67\pm0.04)+i(0.72\pm0.04)$	Constant scattering length analysis for $k_L \lesssim 300$ MeV/c	3
$(-1.63\pm0.07)+i(0.51\pm0.05)$	Constant scattering length analysis for $k_L \lesssim 300$ MeV/c	4
$(-1.65\pm0.04)+i(0.73\pm0.02)$	Effective range K-matrix analysis for $k_L \lesssim 550$ MeV/c	5
$(-1.66\pm0.02)+i(0.69\pm0.02)$	Zero-range K-matrix analysis for $k_L \lesssim 300$ MeV/c	Present calculation

while the inelasticity becomes approximately constant.

Finally, the s-wave $I=0$ $\bar{K}N$ scattering length may be found by evaluating Eq. (5) at threshold. The result is given in Table II, where, again, the K-matrix errors given in I have been used to obtain the error. Table II also gives the results, for comparison, of some previous estimates of this quantity.[3-5] As with the $I=1$ results, the agreement between the various calculations is good.

3. PION-HYPERON INTERACTIONS

One of the advantages of the K-matrix approach is that it allows statements to be made about the pion-hyperon interactions. In this section, we will consider the implications of the results obtained in I for the $\pi\Lambda$ and $\pi\Sigma$ systems.

A. $\pi\Lambda$ Scattering

In terms of the $I=1$ K-matrix elements given in Eq. (6) of I, we may define a matrix of $I=1$ s-wave pion-hyperon amplitudes by

$$\mathbf{F}_1^{YY'}=\mathbf{k}_2^{1/2}\mathbf{Z}_1^{YY'}\mathbf{k}_2^{1/2}(1-i\mathbf{k}_2^{1/2}\mathbf{Z}_1^{YY'}\mathbf{k}_2^{1/2})^{-1}, \quad (7)$$

where

$$\mathbf{Z}_1^{YY'}=\boldsymbol{\gamma}_1+i\boldsymbol{\beta}_1^{\dagger}k(1-ik\alpha_1)^{-1}\boldsymbol{\beta}_1, \quad (8)$$

$$\mathbf{k}_2=\begin{pmatrix} k_\Sigma & 0 \\ 0 & k_\Lambda \end{pmatrix}, \quad (9)$$

$$\boldsymbol{\beta}_1=(\beta_\Sigma \beta_\Lambda), \quad (10)$$

$$\boldsymbol{\gamma}_1=\begin{pmatrix} \gamma_{\Sigma\Sigma} & \gamma_{\Sigma\Lambda} \\ \gamma_{\Sigma\Lambda} & \gamma_{\Lambda\Lambda} \end{pmatrix}, \quad (11)$$

and k_Λ and k_Σ are the magnitudes of the center-of-mass three-momenta in the $\pi\Lambda$ and $\pi\Sigma$ channels, respectively. Using Eqs. (9)–(11) in (8) gives

$$\mathbf{Z}_1^{YY'}\equiv\begin{pmatrix} Z_{\Sigma\Sigma} & Z_{\Sigma\Lambda} \\ Z_{\Sigma\Lambda} & Z_{\Lambda\Lambda} \end{pmatrix} = \begin{pmatrix} \gamma_{\Sigma\Sigma}+H\beta_\Sigma^2 & \gamma_{\Sigma\Lambda}+H\beta_\Lambda\beta_\Sigma \\ \gamma_{\Sigma\Lambda}+H\beta_\Lambda\beta_\Sigma & \gamma_{\Lambda\Lambda}+H\beta_\Lambda^2 \end{pmatrix}, \quad (12)$$

where

$$H(W)=ik/(1-ik\alpha_1). \quad (13)$$

Finally, using Eqs. (12) and (9) in (7) gives

$$F_1^{\Lambda\Lambda}(W)=\frac{ik_\Lambda k_\Sigma Z_{\Sigma\Lambda}^2+k_\Lambda(1-ik_\Sigma Z_{\Sigma\Sigma})Z_{\Lambda\Lambda}}{(1-ik_\Lambda Z_{\Lambda\Lambda})(1-ik_\Sigma Z_{\Sigma\Sigma})+k_\Lambda k_\Sigma Z_{\Sigma\Lambda}^2}. \quad (14)$$

Above the $\pi\Lambda$ threshold we may write

$$f_1^{\Lambda\Lambda}(W)\equiv\frac{F_1^{\Lambda\Lambda}(W)}{k_\Lambda}=\frac{\eta_1^\Lambda(W)\exp[2i\delta_1^\Lambda(W)]-1}{2ik_\Lambda}, \quad (15)$$

where $\delta_1^\Lambda(W)$ and $\eta_1^\Lambda(W)$ are the real part of the s-wave $\pi\Lambda$ phase shift and inelasticity parameter, respectively.

Graphs of $\delta_1^\Lambda(W)$ and $\eta_1^\Lambda(W)$ are shown in Fig. 4 as a function of the incoming-pion laboratory momentum. The real part of the phase shift is positive throughout the low-energy region. The s-wave $\pi\Lambda$ scattering length a_0^Λ may be found by evaluating Eq. (15) at $k_\Lambda=0$. The result is given in Table III. It is of interest to note that the value of a_0^Λ given in Table III is consistent with the current-algebra prediction[6] $a_0^\Lambda=0$.

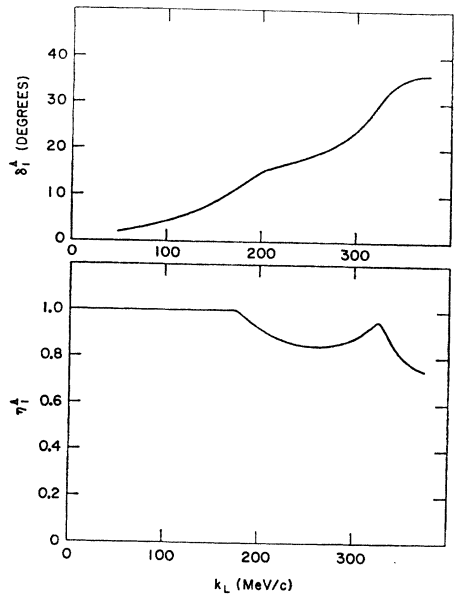

FIG. 4. Phase shift δ_1^Λ and inelasticity η_1^Λ for the $\Lambda\pi$ system in the isotopic-spin $I=1$ channel plotted as a function of the momentum of the π, k_L, in the frame where the Λ is at rest.

[6] See, e.g., A. P. Balachandran, M. G. Gundzik, and F. Nicodemi, *Boulder Lectures in Theoretical Physics* (Gordon and Breach, Science Publishers, Inc., New York, 1967), Vol. 9B.

B. $I=1$ $\pi\Sigma$ Scattering

The s-wave $I=1$ $\pi\Sigma$ amplitude may be found by using Eqs. (9) and (12) in Eq. (7). This gives

$$F_1^{\Sigma\Sigma}(W)=\frac{ik_\Lambda k_\Sigma Z_{\Sigma\Lambda}^2+k_\Sigma(1-ik_\Lambda Z_{\Lambda\Lambda})Z_{\Sigma\Sigma}}{(1-ik_\Lambda Z_{\Lambda\Lambda})(1-ik_\Sigma Z_{\Sigma\Sigma})+k_\Lambda k_\Sigma Z_{\Sigma\Lambda}^2}, \quad (16)$$

and above the $\pi\Sigma$ threshold

$$f_1^{\Sigma\Sigma}(W)\equiv\frac{F_1^{\Sigma\Sigma}(W)}{k_\Sigma}=\frac{\eta_1^\Sigma(W)\exp[2i\delta_1^\Sigma(W)]-1}{2ik_\Sigma}, \quad (17)$$

where $\delta_1^\Sigma(W)$ and $\eta_1^\Sigma(W)$ are the real part of the s-wave $I=1$ $\pi\Sigma$ phase shift and inelasticity parameter, respectively. Graphs of $\delta_1^\Sigma(W)$ and $\eta_1^\Sigma(W)$ are shown in Fig. 5 as a function of the pion laboratory momentum. The real part of the phase shift is positive throughout the low-energy region.

The s-wave $I=1$ $\pi\Sigma$ scattering length may be found by evaluating Eq. (17) at $k_\Sigma=0$ and is given in Table III together with the value obtained by von Hippel and Kim.[5] Unlike the $\bar{K}N$ case, the difference in the predicted values of the scattering length between this calculation and that of Kim is more pronounced, although the signs are the same in both calculations. The difference illustrates the difficulties of obtaining a unique result for pion-hyperon amplitudes from analyses involving only data in the $\bar{K}N$ channel.

C. $I=0$ $\pi\Sigma$ Scattering

The s-wave $I=0$ $\pi\Sigma$ amplitude may be found in terms of the K-matrix elements by analogy with the derivation of Eqs. (4) and (5) of I. It is given by

$$f_0^\Sigma(W)=\frac{A_0^\Sigma(W)}{1-ik_\Sigma A_0^\Sigma(W)}, \quad (18)$$

where

$$A_0^\Sigma(W)=\gamma_0+\frac{i\beta_0^2 k}{1-ik\alpha_0}. \quad (19)$$

Above the $\pi\Sigma$ threshold, $f_0^\Sigma(W)$ may be written

$$f_0^\Sigma(W)=\frac{\eta_0^\Sigma(W)\exp[2i\delta_0^\Sigma(W)]-1}{2ik_\Sigma}, \quad (20)$$

TABLE III. Values of the s-wave pion-hyperon scattering lengths (in F).

Reaction	I	s-wave scattering length (F)	Ref.
$\pi\Lambda\to\pi\Lambda$	1	(0.13 ± 0.07)	Present calculation
$\pi\Sigma\to\pi\Sigma$	1	$(0.28\pm0.03)+i(0.16\pm0.02)$	Present calculation
$\pi\Sigma\to\pi\Sigma$	1	$(0.39\pm0.07)+i(0.14\pm0.03)$	5
$\pi\Sigma\to\pi\Sigma$	0	(0.42 ± 0.03)	Present calculation
$\pi\Sigma\to\pi\Sigma$	0	(1.09 ± 0.23)	5

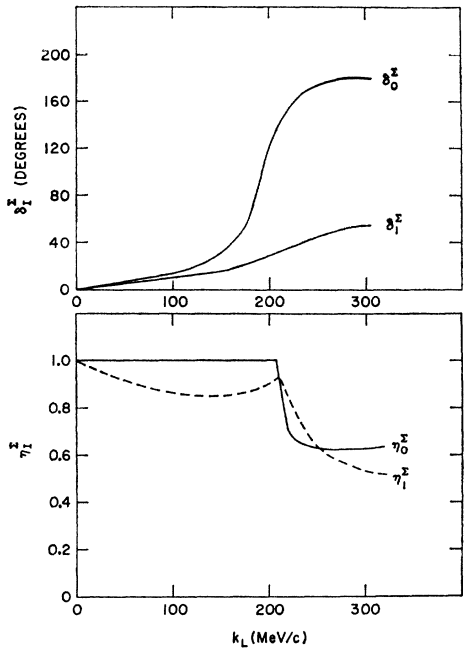

FIG. 5. Phase shift δ_I^Σ and inelasticity η_I^Σ for the $\Sigma\pi$ system in the isotopic-spin $I=1$ and 0 channels plotted as a function of the momentum of the π, k_L, in the frame where the Σ is at rest.

where $\delta_0^\Sigma(W)$ and $\eta_0^\Sigma(W)$ are the real part of the s-wave $I=0$ $\pi\Sigma$ phase shift, and inelasticity parameter, respectively. Graphs of $\delta_0^\Sigma(W)$ and $\eta_0^\Sigma(W)$ as a function of the incoming-pion laboratory momentum are shown in Fig. 5. The amplitude clearly shows an elastic resonance, which we may identify with the $Y_0^*(1405)$. The resonance parameters are shown in Table IV together with, for comparison, other estimates of these quantities. The $Y_0^*(1405)$ may be identified as a pole in the one-channel "reduced K matrix" $A_0^\Sigma(W)$ of Eq. (19) caused by the vanishing of the factor $1-ik\alpha_0$. It confirms that the $Y_0^*(1405)$ is indeed a virtual bound-state resonance of the $\bar{K}N$ system. This pole also occurs in the $I=0$ $\bar{K}N$ amplitude and gives rise to the maximum in $\mathrm{Im}f_0^N(W)$ and the zero in $\mathrm{Re}f_0^N(W)$ seen in Fig. 3. The resonance parameters obtained here are in closer agreement to those obtained in previous "constant scattering length" analyses[3,4] than to those obtained by Kim.[7] In particular, the width of the resonance is found to be far smaller than Kim's value, a fact which has important consequences for the

TABLE IV. Parameters of the $Y_0^*(1405)$ resonance as determined by various $\bar{K}N$ analyses.

Mass (MeV)	Width (MeV)	Ref.	
1410.7 ± 1.0	$37.0\approx3.2$	3	from constant scattering length analyses
1409.6 ± 1.7	28.2 ± 4.1	4	
$1403\ \pm3$	$50\ \pm5$	7	from K-matrix analyses
$1416\ \pm4$	$29\ \pm6$	Present calculation	

[7] J. K. Kim, Phys. Rev. Letters **19**, 1074 (1967).

determination of the kaon-nucleon coupling constants, as we shall discuss below.

Finally, the s-wave $I=0$ $\pi\Sigma$ scattering length which may be found by evaluating Eq. (20) at $k_\Sigma=0$, is shown in Table III together with the value obtained in Ref. 5. The agreement between the two values is only at the 3-standard-deviation level, again illustrating the difficulties in obtaining unique pion-hyperon amplitudes from analyses of this type.

4. DETERMINATION OF $K\Lambda N$ AND $K\Sigma N$ COUPLING CONSTANTS

There has been considerable interest in the values of the $K\Lambda N$ and $K\Sigma N$ coupling constants both because of their importance in phenomenological calculations and because of the implications for higher-symmetry schemes. Early attempts to calculate them from forward KN dispersion relations[8] found values which were far smaller than the πNN coupling constant and were incompatible with $SU(3)$ invariance. Typical results were $g_{K\Lambda N}^2/4\pi\sim 5$ and $g_{K\Sigma N}^2/4\pi\lesssim 2$. Values of this order have also been found in analyses of kaon photoproduction reactions.[9] However, it was pointed out by Rood[10] that the determination of the coupling constants from forward-dispersion-relation sum rules was particularly sensitive to the integrals over the unphysical region occurring in $\bar{K}N$ scattering, and it is precisely this region where the constant scattering length parametrization is expected to be poor. By making some estimates for the K-matrix parameters, Rood[10] showed that appreciable changes could be produced in the coupling constants by an alternative parametrization of the unphysical region.

Recently, Kim[11] has reevaluated two forward-dispersion-relation sum rules, using the results of his K-matrix analysis, and found values $g_{K\Lambda p}^2/4\pi=13.5\pm 2.1$ and $g_{K\Sigma p}^2/4\pi=0.2\pm 0.4$. The value of $g_{K\Lambda p}$ is far larger than previous estimates and is, moreover, now compatible with $SU(3)$ invariance. In view of the importance of this result, it is desirable to have an independent calculation of the coupling constants. Thus, in this section, we will evaluate the coupling constants from the forward-dispersion-relation sum rules using the K-matrix parameters obtained in I, and, in addition, discuss the difficulties involved in making a reliable calculation at this time.

If we denote by $f_\pm^N(\nu)$ the forward amplitude for $K^\pm N$ ($N=n$, p) scattering at a total kaon laboratory energy ν, and by $\sigma_\pm^N(\nu)$ the corresponding total cross section, then the basic unsubtracted dispersion relation for $f_\pm^N(\nu)$ may be written

$$\mathrm{Re}f_\pm^N(\nu)=\sum_Y \frac{R_Y^N}{\nu_Y\pm\nu}+\frac{1}{\pi}\int_{\bar{\nu}}^m d\nu'\frac{\mathrm{Im}f_-^N(\nu')}{\nu'\pm\nu}+\frac{P}{2\pi^2}\int_m^\infty d\nu' k'\left(\frac{\sigma_+^N(\nu')}{\nu'\pm\nu}+\frac{\sigma_-^N(\nu')}{\nu'\pm\nu}\right), \quad (21)$$

where m is the mass of the kaon,

$$\nu_Y=(M_Y^2-M^2-m^2)/2M,$$

and[12]

$$R_Y=\frac{(M_Y-M)^2-m^2}{4M^2}\frac{g_{KYN}^2}{2\pi}.$$

The kaon laboratory momentum is k'; M is the mass of the nucleon; and M_Y and g_{KYN} are the masses and couplings of the hyperons Y (Λ and Σ) to the $\bar{K}N$ channel. The first integral in Eq. (21) represents the contribution from the unphysical region in $\bar{K}N$ scattering, and the lower limit $\bar{\nu}$ is taken to correspond to the $\pi\Lambda$ or $\pi\Sigma$ threshold, depending on whether $I=1$ or $I=0$ states are involved.

The integrals in Eq. (21) are not expected to converge as they stand. However, a linear combination which should converge is

$$F_N^-\equiv\tfrac{1}{2}[f_-^N(\nu)-f_+^N(\nu)]. \quad (22)$$

Thus, from (21) and (22) we have

$$\mathrm{Re}F_N^-=\nu\sum_Y\frac{R_Y^N}{\nu_Y^2-\nu^2}+\frac{\nu}{\pi}\int_{\bar{\nu}}^m d\nu'\frac{\mathrm{Im}f_-^N(\nu')}{\nu'^2-\nu^2}+\frac{\nu}{4\pi^2}P\int_m^\infty d\nu' k'\frac{\sigma_-^N(\nu')-\sigma_+^N(\nu')}{\nu'^2-\nu^2}. \quad (23)$$

In order to isolate the Λ-pole term, we shall work with the amplitude

$$T(\nu)\equiv F_n^-(\nu)-2F_p^-(\nu), \quad (24)$$

which has no $I=1$ contributions in the $\bar{K}N$ channel. Thus, both the Σ and $Y_1^*(1385)$ contributions are removed. Evaluating Eq. (24) at threshold $\nu=m$ then gives

$$\frac{M+m}{4M}(3a_1-a_0-2\bar{a}_0)=\frac{-m[(M_\Lambda-M)^2-m^2]}{2M^2(\nu_\Lambda^2-m^2)}\frac{g_{K\Lambda p}^2}{4\pi}-\frac{m}{\pi}\int_{\nu_{\pi\Sigma}}^m d\nu'\frac{\mathrm{Im}\bar{f}_0(\nu')}{\nu'^2-m^2}+\frac{m}{4\pi^2}P\int_m^\infty d\nu' k'\times\frac{\sigma_-^n(\nu')-\sigma_+^n(\nu')-2\sigma_-^p(\nu')+2\sigma_+^p(\nu')}{\nu'^2-m^2}, \quad (25)$$

[8] See, e.g., G. H. Davies, N. M. Queen, M. Lusignoli, M. Restignoli, and G. Violini, Nucl. Phys. **B3**, 616 (1967), and earlier references quoted therein.

[9] See, e.g., N. F. Nelipa, Nucl. Phys. **82**, 680 (1966), and earlier references quoted therein.

[10] H. P. C. Rood, Nuovo Cimento **50A**, 493 (1967).

[11] J. K. Kim, Phys. Rev. Letters **19**, 1079 (1967).

[12] When comparing values of g_{KYN} it should be noted that some authors replace the factor $4m^2$ in R_Y by $4m_Ym$.

where a_I and $\bar{a}_I$ ($I=0$, 1) are s-wave scattering lengths for KN and $\bar{K}N$ scattering, respectively, and $\mathrm{Im}\bar{f}_0(\nu)$ denotes the imaginary part of the $I=0$ $\bar{K}N$ forward scattering amplitude.

We shall rewrite (25) as a sum rule for $g_{K\Lambda p}^2/4\pi$ in the form

$$\frac{g_{K\Lambda p}^2}{4\pi}=\sum_{i=1}^{11} A_i, \tag{26}$$

where the various A_i correspond to the following parts of Eq. (25):

A_1: contributions from the scattering lengths;

A_2: s-wave $I=0$ $\bar{K}N$ unphysical region and scattering below 300 MeV/c;

A_3: K^-n scattering in the range 300–800 MeV/c;

A_4: K^-p scattering in the range 300–800 MeV/c;

A_5: K^+n scattering in the range 0–800 MeV/c;

A_6: K^+p scattering in the range 0–800 MeV/c;

A_7: K^-n scattering in the range 0.8–5.0 BeV/c;

A_8: K^-p scattering in the range 0.8–5.0 BeV/c;

A_9: K^+p scattering in the range 0.8–5.0 BeV/c;

A_{10}: K^+n scattering in the range 0.8–5.0 BeV/c;

A_{11}: total asymptotic region above 5 BeV/c.

The contributions have been separated in this way to exhibit the importance of the various regions, not all of which are known with the same degree of accuracy. The value of $g_{K\Sigma^0 p}^2$ may similarly be found from the sum rule for $F_n^-(m)$, i.e.,

$$\frac{M+m}{4M}(2\bar{a}_1-a_0-a_1)=\frac{m[(M_\Sigma-M)^2-m^2]}{4M^2(\nu_\Sigma^2-m^2)}\times\frac{g_{K\Sigma^- n}^2}{4\pi}+\frac{m}{\pi}\int_{\nu_{\pi\Lambda}}^{m}d\nu'\frac{\mathrm{Im}\bar{f}_1(\nu')}{\nu'^2-m^2}+\frac{m}{4\pi^2}P\int_m^\infty d\nu' k'\frac{\sigma_-^n(\nu')-\sigma_+^n(\nu')}{\nu'^2-m^2}. \tag{27}$$

Using the charge-independent result $g_{K\Sigma^- n}^2=2g_{K\Sigma^0 p}^2$, we will write the above as a sum rule for $g_{K\Sigma^0 p}^2/4\pi$ in the form

$$\frac{g_{K\Sigma^0 p}^2}{4\pi}=\sum_{i=1}^{8} B_i, \tag{28}$$

where the various B_i are

B_1: contributions from the scattering lengths;

B_2: s-wave $I=1$ unphysical region and scattering below 300 MeV/c;

B_3: $Y_1^*(1385)$ contribution to the unphysical region;

B_4: K^-n scattering in the range 300–800 MeV/c;

B_5: K^-n scattering in the range 0.8–5.0 BeV/c;

B_6: K^+n scattering in the range 0–800 MeV/c;

B_7: K^+n scattering in the range 0.8–5.0 BeV/c;

and

B_8: total asymptotic region above 5 BeV/c.

We shall first discuss the evaluation of $K\Lambda N$ coupling constant from Eq. (26): The term A_1 was calculated using the values of a_1 and a_0 from the experiments of Refs. 13 and 14, and using the value of $\bar{a}_0$ obtained from the results of our K-matrix analysis given in Table II. The term A_2 was similarly calculated using the results of the K-matrix analysis. The values of A_1 and A_2 with their errors are given in Table V. The value of A_3 is poorly known because of the lack of total cross-section measurements for K^-n scattering in the region below 600 MeV/c. In order to evaluate this term, therefore, we have smoothly continued the value of σ_-^n at 300 MeV/c as predicted by the results of the K-matrix analysis to the value at 600 MeV/c as measured by Bugg *et al.*[15] The resulting value of A_3 is given in Table V and is fortunately small. The values of A_4–A_{10} may be found using published values for the relevant total cross sections,[16] and are given in Table V. Finally, the asymptotic region was evaluated using the Regge-pole model of Phillips and Rarita.[17] These authors give no errors on their Regge parameters, but since most of the contribution comes from the region below 25 BeV/c, for which there are measured cross sections, we have

TABLE V. Contributions to $g_{K\Lambda p}^2/4\pi$ from the different parts of the dispersion relation.

	Contribution to $g_{K\Lambda p}^2/4\pi$	Value	Error
A_1	Scattering lengths	−18.2	0.6
A_2	s-wave $I=0$ $\bar{K}N$ below 300 MeV/c and unphysical region	35.1	1.7
A_3	K^-n 300–800 MeV/c	2.7	0.1
A_4	K^-p 300–800 MeV/c	− 9.1	0.2
A_5	K^+n 0–800 MeV/c	− 1.5	0.1
A_6	K^+p 0–800 MeV/c	3.7	0.2
A_7	K^-n 0.8–5.0 BeV/c	5.9	0.0
A_8	K^-p 0.8–5.0 BeV/c	−14.4	0.0
A_9	K^+p 0.8–5.0 BeV/c	7.7	0.0
A_{10}	K^+n 0.8–5.0 BeV/c	− 4.2	0.0
A_{11}	Asymptotic region above 5.0 BeV/c	− 2.7	0.1
	Total	5.0	1.9

[13] S. Goldhaber, W. Chinowsky, G. Goldhaber, W. Lee, T. O'Halloran, T. F. Stubbs, G. M. Pjerrou, D. H. Stork, and H. K. Ticho, Phys. Rev. Letters **9**, 135 (1962).

[14] V. J. Stenger, W. E. Slater, D. H. Stork, H. K. Ticho, G. Goldhaber, and S. Goldhaber, Phys. Rev. **134**, B1111 (1964).

[15] D. V. Bugg, R. S. Gilmore, K. M. Knight, D. C. Salter, G. H. Stafford, E. J. N. Wilson, J. D. Davies, J. D. Dowell, P. M. Hattersley, R. J. Homer, A. W. O'Dell, A. A. Carter, R. J. Tapper, and K. F. Riley, Phys. Rev. **168**, 1466 (1968).

[16] A complete list of references may be found in Ref. 8; see also Ref. 15.

[17] R. J. N. Phillips and W. Rarita, Phys. Rev. **139**, B1336 (1965).

TABLE VI. Contributions to $g_{K\Sigma^0 p}^2/4\pi$ from the different parts of the dispersion relation.

	Contribution to $g_{K\Sigma^0 p}^2/4\pi$	Value	Error
B_1	Scattering lengths	1.5	3.0
B_2	s-wave $I=1$ below 300 MeV/c and unphysical region	2.9	0.2
B_3	$Y_1^*(1385)$	<0	
B_4	K^-n 300–800 MeV/c	-1.4	0.2
B_5	K^-n 0.8–5.0 BeV/c	-3.0	0.1
B_6	K^+n 0–800 MeV/c	0.8	0.1
B_7	K^+n 0.8–5.0 BeV/c	2.1	0.0
B_8	Asymptotic region above 5 BeV/c	-0.8	0.1
	Total	<2.1	3.0

used the quoted errors on these latter quantities[16] to estimate an error on A_{11}. The value of A_{11} and its error is given in Table V.

As remarked in Sec. 3 C, the width of the Y_0^* obtained in the present analysis is far smaller than that obtained by Kim.[7] Since the unphysical region gives the largest contribution to the sum rule for $g_{K\Lambda p}^2$ (see Table V), this implies that the value of the Λ coupling constant will be smaller than that obtained by Kim.[11] This is confirmed by our final result given in Table V.

We have also estimated the value of $g_{K\Sigma^0 p}^2$ from Eq. (28). The terms B_1–B_2 and B_4–B_8 may be evaluated following the evaluation of the equivalent terms in Eq. (26): The only other term is due to the $Y_1^*(1385)$, and here all we known for certain is that its contribution to Eq. (28) is negative. Using this fact alone leads to the results shown in Table VI. We conclude that $g_{\Sigma K^0 p}^2 \lesssim 2.1$, but the cancellations previously observed in Table V for the $K\Lambda N$ coupling constant are as severe for the $K\Sigma N$ coupling constant and suggest that an alternative relation should be used if the value of this coupling constant is to be accurately known.

The question that remains is whether the $K\Lambda N$ coupling constant obtained in this calculation is really incompatible with that obtained by Kim. Although at first sight it appears that they are indeed incompatible, one must remember that the errors quoted in *both* calculations are only statistical. If, for example, the term A_2 in Table V was subject to a systematic error which increased its value by only 10%, then $g_{K\Lambda p}^2/4\pi$ would become 8.7 ± 2.0. Similar considerations apply to the evaluation of the unphysical region in Kim's calculation, although a 10% variation there would cause a larger change in the value of the coupling constant because of the larger contribution of this region.

A possible source of such systematic errors could easily be the distance of the necessary extrapolations. For example, the analysis of I shows that effective range terms are not required in the K matrix for K^- momenta below $\sim$300 MeV/c. Thus, the effective range terms in Kim's analysis are determined by the data in the range 300–550 MeV/c, which corresponds to center-of-mass energies of 1490–1585 MeV. However, these terms are used in the sum rules in the unphysical region, i.e., 1255–1435 MeV, and thus the extrapolation is typically of the order of 190 MeV, which is considerable. Thus, there may easily exist systematic errors in both the present calculation and that of Kim[11] which could remove the apparent inconsistencies in the values obtained for $g_{K\Lambda p}^2$. We must conclude, therefore, that our present knowledge of the KYN coupling constant extends only to the very weak statements that $3 \lesssim g_{K\Lambda p}^2/4\pi \lesssim 15$ and $g_{K\Sigma^0 p}^2/4\pi \lesssim 2.1$.

5. SUMMARY AND CONCLUSIONS

We have used the K-matrix parameters obtained from our analysis of low-energy K^-p data[1] to examine the behavior of the $\bar{K}N$, $\pi\Lambda$, and $\pi\Sigma$ s-wave amplitudes and, in addition, to evaluate the kaon-nucleon coupling constants from forward-dispersion-relation sum rules. The results show that it is not possible at present to calculate with any accuracy the values of these coupling constants.

How can one decide between different K-matrix solutions? One method that has been proposed by Queen *et al.*[18] uses sum rules derived from the condition that the coupling constants should be energy-independent. All parametrizations used to date apparently fail to satisfy these sum rules, but again the role of systematic errors could well be important. It is clear that before an improvement in phenomenological analyses can be made, more accurate data are required in the low-energy region. In view of the implications that this has for the evaluation of the kaon-nucleon coupling constants, experiments in this region are highly desirable.

[18] N. M. Queen, S. Leeman, and F. E. Yeomans, Birmingham Report, 1968 (unpublished).